

# USING X-RAYS TO CHARACTERIZE THE PROCESS OF SELF-ASSEMBLY IN REAL TIME

A.G. Richter,<sup>(a)</sup> C.-J. Yu, A. Datta,<sup>(b)</sup> J. Kmetko and P. Dutta\*

Dept. of Physics & Astronomy, Northwestern University, Evanston, IL 60208, USA

## ABSTRACT

We have performed *in situ* x-ray reflectivity studies of the growth of octadecyltrichlorosilane (OTS) monolayers on oxidized Si(111) from solutions in heptane. We find that for all concentrations, the film grows through the formation of islands of vertical molecules. The coverage follows a simple Langmuir form as a function of time, except for very low concentration solutions at early times, where a time offset is required to fit the curve. We have also examined films removed from solution, and we find that rinsing removes molecules and causes the remaining molecules to tilt. Thus, samples studied using the “interrupted growth” technique are not representative of the actual growth process.

<sup>(a)</sup> Present address: Argonne National Laboratory, Argonne, IL 60439, USA

<sup>(b)</sup> Present address: Saha Institute of Nuclear Physics, Calcutta 700064, India

\* Corresponding author. Phone +1-847-491-5465; fax +1-847-491-9982; e-mail [pdutta@northwestern.edu](mailto:pdutta@northwestern.edu)

## Introduction

Despite their technological promise and more than a decade of extensive research, many fundamental questions still remain concerning the growth of self-assembled monolayers (SAMs). Until recently, all of the studies of solution-grown SAMs that examined incomplete films were performed using an interrupted growth technique [1-14]. Substrates were dipped in solution and then after a certain amount of time, the growth was quenched. The samples were then rinsed and characterized *ex situ*. This method provides some opportunity for morphological changes in the film, as the local environment is radically altered during the growth. Therefore, this technique may not reliably indicate what is actually occurring during deposition.

A number of different growth modes for SAM formation have been hypothesized. The simplest cases are island growth and “uniform” growth (also called homogeneous growth). Island growth would proceed by formation of ordered islands of adsorbed molecules. The structure of the islands could also change over deposition time, perhaps tilting over at first, and then becoming vertical later. The other extreme is uniform growth, in which growth proceeds by formation of a homogeneous layer of physisorbed and chemisorbed molecules that tilt over to form a film of high density. As the coverage increases, the molecules stand up to accommodate newly adsorbed molecules. Another growth mode possibility could be randomly deposited, vertically oriented molecules, which would proceed by adsorption of molecules from solution at random positions but without the (large) change in tilt over deposition time.

By performing interrupted growth experiments, some authors [6,8-12,15] have concluded that OTS grows in the form of islands. Some of these experiments show islands surrounded by a “gas” of physisorbed molecules; other show these regions to be void of molecules. Other authors [1,3,4,16] have concluded that the preferential mode is uniform growth. Growth may be a combination of these two modes [8,15,17], the islands may be composed of tilted molecules [5], or there may be some other growth mode [14]. Even more recent *in situ* studies [18-24] do not present a consistent picture.

Using X-ray reflectivity for growth studies has only recently become viable with the building of second and third generation synchrotrons. X-rays produced by synchrotrons are particularly useful for probing internal interfaces in many cases. First, measuring the reflectivity requires that a large number of photons be incident on the surface or interface at small incident angles, which requires a small beam spot at the sample; synchrotrons provide this. Second, the X-ray energy can be varied; using higher energies allows the X-rays to penetrate to an internal interface. Third, X-rays are largely non-destructive and thus allow characterization of a process such as self-assembly without interrupting or affecting the process. We show here how X-rays may be used to study the process of self-assembly directly at a substrate-solution interface.

### Experimental details

The intensity of an electromagnetic wave reflected off an ideally sharp (step-function) interface can be derived straightforwardly from Maxwell's equations. The result is called the Fresnel Reflectivity

$$R_F(q) = \left| \frac{q - \sqrt{q^2 - q_c^2}}{q + \sqrt{q^2 - q_c^2}} \right|^2.$$

Where  $q_c$  is the critical angle for total reflection. For  $q > 3q_c$ ,  $R_F(\theta) \approx \left( \frac{\sin \theta_c}{2 \sin \theta} \right)^4$ , which means that the reflected intensity drops very rapidly past the critical angle.

For any real system, there is some non-step-function electron density  $\rho(z)$ , averaged over the x and y directions, that describes a film's profile. For x-rays to reflect, rather than to merely scatter isotropically, there must be a gradient in the electron density. A film that has several different layers will also have several interfaces. In the Born Approximation, the reflectivity  $R(q)$  is related to the Fresnel reflectivity by [25]

$$\frac{R(q)}{R_F(q)} = \left| \frac{1}{\rho_0} \int \frac{d\langle \rho(z) \rangle}{dz} e^{iqz} dz \right|^2$$

where  $\rho_0$  is the electron density of the semi-infinite bulk and  $\langle\rho(z)\rangle$  is the electron density averaged in the x-y plane over the X-ray coherence length. This form explicitly shows that the reflection primarily occurs at interfaces, where the electron density gradient is large. This expression also shows why in situ X-ray reflectivity is more difficult than the same experiment ex situ. The density difference between an SA monolayer and air, and thus the density gradient in the z-direction, is much larger than those between an SAM and a solvent.

Fig. 1 illustrates the role of the solvent by comparing calculated reflectivity data from an uniform OTS SAM on silicon with three different solvents. Toluene has almost exactly the same density as OTS and thus the reflectivity is almost featureless. Heptane has a slightly lower density than OTS and therefore the features are more clearly visible, although an ex situ sample (in air) would show much deeper minima. On the other hand,  $\text{CCl}_4$  has a higher density than OTS; it shows the clearest features of the three solvents considered (note that the locations of the minima in heptane are the locations of the maxima with  $\text{CCl}_4$ ; this is because the sign of the density gradient has changed). What is not included in this calculation, however, is the absorption and random background scattering due to the solvent;  $\text{CCl}_4$  is more dense and so attenuates the beam and adds a higher background. We found heptane to be well suited for these experiments, and the data reported below are all obtained with heptane as solvent. We used an X-ray energy of 11 KeV or higher to reduce absorption in the solvent. In spite of these steps, our reflectivity data are indistinguishable from background by about 0.5 to 0.6  $\text{\AA}^{-1}$ , while ex situ reflectivity studies can go to twice that or more. Each reflectivity scan shown in this paper took 20-60 minutes to complete.

Because of the “phase problem” of x-ray scattering (one measures intensities rather than amplitudes), the electron density profile  $\langle\rho(z)\rangle$  cannot be calculated directly from the reflectivity. We have to assume a model for the profile and then fit the reflectivity curve by varying model parameters. A typical model is the Gaussian-step model [1], in which the regions between interfaces are assumed to be of uniform density, and the interfaces are modeled as error-functions.

The Si(111) substrates were cleaned with piranha etch, followed by RCA treatment for hydroxylation. They are then rinsed with water again and stored under water until needed. For self-assembly, OTS solutions are usually made in cyclohexane or toluene, but we used heptane as our solvent because it has a low electron density and it can be made very anhydrous. To minimize water vapor, all work was done in a glovebag filled with nitrogen. The OTS solutions were made and kept in the glovebag in a presilanized, covered, glass, 100 ml container for a maximum of 4 days. Solutions of varying concentrations were made, ranging from 0.1% (2.5 mM) to  $10^{-4}$ % (2.5  $\mu$ M) by volume. No visible condensation of the OTS occurred at any concentration while the solution was being stored or used. While care was taken to ensure control over concentration levels, reported concentrations should be taken to be only accurate to within  $\pm 30\%$ . The samples were at room temperature (not separately temperature-controlled).

The *in situ* cell is based on a design by You and Nagy [26]. Figure 2 shows a schematic diagram of the cell. The central piece is a 5 mm thick Teflon slab that has a cut-out section. The silicon substrate is held in place under tabs in the Teflon and by nylon screws. The cut-out also provides a cavity for about 6 ml of solution. The Teflon piece is sandwiched between two 0.01-inch thick beryllium plates. Beryllium is a very low-z material and so does not absorb x-rays greatly; the two Be plates together lower the intensity by about 5% at 11 keV. This assembly is further sandwiched between two stainless steel pieces that provide structural support. Windows in the stainless steel pieces allow x-rays to pass through, and are constructed to have a vertical acceptance angle of approximately  $60^\circ$ , and a horizontal acceptance angle of about  $120^\circ$ . The windows measure 1 cm by 1 cm, and the substrate is positioned such that the surface is flush with the bottom of the window. Solution is drawn into and removed from the chamber via Teflon inlet and outlet tubes in the inner Teflon piece using syringes with Luer lock connectors. Assembly of the cell and introduction of the solution were performed in the glovebag. For *in situ* studies, the substrate was first examined under clean heptane to obtain a reference scan. Then, the solution was introduced at time zero via syringe.

After film formation, the samples were removed, either from the solution container or from the *in situ* sample holder. Samples to be re-studied *ex situ* were rinsed several times with clean heptane, then rinsed repeatedly with methanol, and finally with ethanol. Samples were removed from the glovebag while in ethanol, then blown dry with nitrogen. All samples were hydrophobic after removal from solution as evidenced by large water contact angles.

## Results

### (i) *in situ* Growth Studies

Our earliest time-dependence studies were reported in Ref. 27. We used a  $10^{-4}\%$  concentration ( $2.5 \mu\text{M}$ ) of solution to slow the growth down to  $\sim 20$  hours and get more than ten reflectivity scans lasting 45-60 minutes each during film growth. This allowed us to treat each individual scan as close to a “snapshot.” We found that (a) the thickness of the film always remained constant at the expected thickness of a complete monolayer; (b) the monolayer electron density increased continuously until it leveled off after  $\sim 20$  hours. Thus the molecules are always vertical when deposited, but the monolayer fills in with time. This is different from the ‘uniform’ growth model, in which the density of the incomplete film is close to that of the complete film but the thickness increases with deposition time. When the film is in contact with the solution, interactions with the solvent presumably help to keep the adsorbed molecules vertical. We do not know why the uniform mode is observed in some interrupted-growth studies [1,3,4,16] but not in others [6,8-12,15]

We found no evidence for the existence of regions of different thicknesses (which would smear the reflectivity curves and make them difficult to fit with a simple density profile).

The small density gradient at the film-solution interface does not allow us to use the interface width parameter as a sensitive probe of monolayer uniformity; however, the fits are sensitive to large changes in the interface width ( $> 2 \text{ \AA}$ ), which we do not detect. This argues against a picture of randomly deposited molecules, which would require that a partially-depos-

ited monolayer have a very rough monolayer-solution interface. We therefore conclude that this system undergoes ‘island-type’ growth, with domains of the same thickness.

Separately, we made an attempt to find the in-plane diffraction peak, in the hope of looking at its time evolution. We put a sample into 0.15% solution for 15 hours, rinsed it, and scanned under helium from  $q_{xy} = 1.3$  to  $1.7 \text{ \AA}^{-1}$  at  $q_z = 0.1 \text{ \AA}^{-1}$ . Only a hint of a peak was observed at  $q_{xy} = 1.5 \text{ \AA}^{-1}$ , the height being only 3 error bars above background. Figure 3 is the combination of 3 scans with 30 seconds per point. A fit to a Lorentzian gives a FWHM of  $0.049 \text{ \AA}^{-1}$ , corresponding to a correlation length of  $40.5 \text{ \AA}$ , very similar to that found by Tidswell [4]. We did not perform a  $q_z$  scan. Since this *ex situ* peak is so weak, we did not attempt to perform an *in situ* diffraction scan.

Most of the published work on the OTS/Si system was done with millimolar concentrations. Thus it is possible to speculate that there could be a difference in growth mode between our low concentrations and those used by others. For this reason, we made several *in situ* studies at various concentrations. By streamlining the alignment and scanning processes, and by reducing the number of data points and the collection time for each point, we have been able to follow the growth at higher concentrations [28]. *In situ* studies were performed at various concentrations, ranging from  $10^{-1}\%$  to  $10^{-4}\%$  by volume (2.5 mM to 2.5  $\mu\text{M}$ ). All of the reflectivity scans showed similar behavior. Figure 4 shows *in situ* reflectivity curves for a few samples, all at lower concentrations. The high concentration samples ( $> 10^{-2}\%$ ) grew so quickly that good fits to the curves could not be obtained until late in the growth when changes in the film morphology slowed. Figure 4 also shows the coverage as a function of deposition time for these samples. In each case, the density increases with time, while the thickness (not shown) stays constant.

One of the simplest and most common growth modes is Langmuir kinetics, in which the rate of coverage increase is proportional to the uncovered space on the surface.

$$\frac{d\theta}{dt} = F(1 - \theta)$$

which leads to

$$\theta = 1 - e^{-t/\tau}$$

where  $F$  is the adsorption rate, and  $\tau$  is the growth timescale ( $=1/F$ ). In this model, the adsorbed molecules are assumed to be non-interacting, merely serving to block molecules in solution from landing on the surface. We attempted to fit Langmuir curves to our growth curves. We converted the density to coverage using the equation

$$\theta = \frac{\rho_{film} - \rho_{solution}}{\rho_{complete} - \rho_{solution}}$$

where  $\rho_{solution}$  is  $0.34\rho_{Si}$  and  $\rho_{complete}$  is found by fitting the density data to a modified Langmuir function. The curves from the lowest concentrations show a deviation from a Langmuir shape at early times. We cannot adequately fit these curves unless we exclude these points from the fit and allow for a time-offset before Langmuir kinetics begin. If we do so, we get quite good fits to the rest of the data using the form

$$\theta = 1 - e^{-(t-t_0)/\tau}$$

where  $t_0$  is the time-offset. Figure 4 shows some of these fits and lists the fitted parameters, and Table I contains the Langmuir fit parameters for all samples studied. The lowest concentration behavior [27] is not anomalous; rather, at all solution concentrations studied, the molecules are vertical during deposition.

As is to be expected, as the concentration increases, there is a general decrease in the growth timescales (an increase in the growth rate). However, we do not observe a monotonic decrease. This is most likely due to the fact that we do not have adequate control over all the important chemistry parameters, such as substrate conditions, solution water levels, humidity, and temperature. It is well documented that a variation in any of these parameters leads to a variation in the speed of film formation and in some cases, the quality of the film [5,8,11,15,16,31-36].

Because of our limited time resolution, we cannot discern why there is a deviation from Langmuir kinetics at early times at low concentrations. We have at best two data points in this region, and the size of the error bars rules out any unambiguous complicated functional fit.

There seems to be an inverse relationship between the required time-offset and the growth rate,

implying that the offset is due to a process that requires a certain number of molecules before switching to Langmuir kinetics. This could be the initial nucleation of the film, which would presumably be slower with a lower impingement rate (concentration).

Except for deviations at short times, the growth does appear to follow Langmuir kinetics. However the saturated exponential form of Langmuir kinetics can be observed for more complicated interactions in limiting cases. The adsorption rates ( $1/\tau$ ) that we find range from  $4.4 \times 10^{-5} \text{ s}^{-1}$  for the slowest growing sample (2.5  $\mu\text{M}$ ) to  $4.5 \times 10^{-4} \text{ s}^{-1}$  for the fastest (0.15 mM). This compares favorably with the value found by Doudevski et al. [22] for octadecylphosphonic acid (OPA) on mica of  $8.1 (\pm 0.5) \times 10^{-5} \text{ s}^{-1}$  for a solution concentration of 0.1 mM. Vallant *et al.* in a recent paper [18] reported using *in situ* Attenuated Total Reflection Infrared Spectroscopy (ATR-IR) to study the growth on OTS on silicon and has also found that the coverage follows the Langmuir adsorption model. The adsorption rate that they measure for a 1 mM solution (with a water concentration of 2.2 mM) is  $2.8 \times 10^{-4} \text{ s}^{-1}$ , again very similar to the value we obtained (see Table I).

In their study of a different SAM system, alkylthiols on gold, Eberhardt *et al.* also observe Langmuir growth after an initial delay [37]. In their case, this offset is due to an initial phase of lying-down molecules which does not contribute to the signal used to calculate the coverage of molecules in the fully formed film phase. While we are insensitive to molecules that are lying down because of resolution constraints, we do observe that even at these early times some proportion of molecules are vertical, so it is unlikely that our system undergoes a similar phase transition as for the thiol/Au system.

#### (ii) Comparison with ex situ studies

In order to address the inconsistencies between our *in situ* study derived island growth result and those interrupted growth studies that display uniform growth, a comparison between the structure of a film while in solution and when removed from solution was made in three ways. The first procedure, also the simplest, was to compare the final *in situ* reflectivity curve with one taken

after the same sample was removed from the cell and rinsed and then placed under helium. For the second procedure, a sample's growth was followed *in situ* and then the sample was rinsed and re-immersed in heptane and rescanned. And the third procedure was the preparation of a series of "interrupted growth" samples by removing substrates from solution before complete monolayer formation could occur and then scanning under helium.

The first procedure was performed numerous times with many different *in situ* examined samples. *In situ* scans were usually taken until no change could be seen in the reflectivity curve, after which it was assumed that the growth was finished. Then the samples were removed and rinsed. In all cases, the fits to the reflectivity curve showed that the thickness and the density were lower after rinsing than during the last *in situ* scan [28].

The second procedure was performed to determine what would happen after placing a quenched and rinsed sample back under solvent (Fig. 5). After following the growth of sample S7 *in situ* until it appeared to be finished, the standard rinsing procedure was used. Then, the sample was put back under heptane and examined. Additionally, a sample, S8, that was prepared with the same solution and for the same amount of time but which had not been previously exposed to x-rays was treated in the same manner. Figure 5 shows the reflectivity curves and the electron density profiles obtained by fitting. It is clear that after rinsing, the thickness and density of the film decrease somewhat and that placing under heptane does not return the thickness to its previous value. A fit to the reflectivity curve of S7 taken under heptane gives an electron density of  $0.410 \rho_{Si}$  and a thickness of  $23.64 \text{ \AA}$  compared to  $0.438 \rho_{Si}$  and  $24.44 \text{ \AA}$  for the final *in situ* scan. It is also clear that the loss of material from the film is not an effect of x-ray damage.

For the "interrupted growth" study, four clean substrates were placed into an OTS solution ( $2 \times 10^{-3}\%$  by volume,  $50 \mu\text{M}$ ) and then removed one by one, allowing several hours to lapse between each sample removal. The samples were rinsed in the standard way and then scanned under a helium environment. We found that the minimum in the reflectivity shifts to progressively lower and lower  $q$  values, directly indicating that the film gets thicker over deposi-

tion time, consistent with earlier reports [1,3,4,16,18,31]. Also, the minima get deeper, indicating that the film increases in density.

The first two comparison methods show that quenching the growth before full film formation causes the thickness and the density to decrease. Rinsing also appears to cause an irreversible process to occur, as re-immersion in solvent does not restore the film to its pre-rinsed thickness. Combining these two findings leads us to propose that the solvent molecules help keep the adsorbed molecules vertical and that rinsing the film causes some of the non-cross-linked molecules to be removed from the film, creating free volume. Some of the molecules then tilt over, lowering the thickness. Several studies have proposed that the OTS molecules do not fully cross-link until late in the deposition process [7,16,38,39], that the degree of hydrolysis depends on water content of the solution [40], and that even in a fully formed film, many siloxane groups are still present, indicating that not all of the molecular siloxyl groups have cross-linked [16]. Furthermore, there appears to be only minimal direct attachment of OTS molecules to the surface [16,32,36,40,41], meaning that the molecules must attach to one another to form a complete film. XRR is sensitive to the presence of both the chemisorbed and physisorbed molecules and does not differentiate between the two if both species have similar tilt angles. The act of rinsing an incomplete film may then remove the physisorbed molecules which are only held in place by hydrogen bonding to neighbors and possibly to the postulated water layer.

The interrupted growth study confirms our suspicions of the inconsistencies between our *in situ* results and the results of other groups' studies that report uniform growth. Our *in situ* observation of island growth was not due to various unquantified differences between different groups in experimental conditions and procedures, but rather it is the act of quenching and rinsing that causes this discrepancy; the actual mode of growth while in solution is through the formation of uniformly thick islands. Substrate and solution water level differences, and temperature and cleanroom conditions, can certainly alter the film morphology and this may be partially responsible for some of the different growth mode observations. However, our study shows that even with the same growth conditions that give rise to island growth and the formation of well-

packed complete monolayers, removal from solution, rinsing, and drying does cause a change in the SAM.

### **Acknowledgments**

This research was supported by the US Department of Energy under Grant DE-FG02-84ER45125. It was performed at Sector 10 (MRCAT) of the Advanced Photon Source, and at the National Synchrotron Light Source; these facilities are also supported by the US Department of Energy.

**References**

1. I. M. Tidswell, B. M. Ocko, and P. S. Pershan, *Phys. Rev. B* 41, 1111 (1990).
2. M. Pomerantz, A. Segmüller, L. Netzer, and J. Sagiv, *Thin Solid Films* 132, 153 (1985).
3. S. R. Wasserman, G. M. Whitesides, I. M. Tidswell, B. M. Ocko, P. S. Pershan, and J. D. Axe, *J. Am. Chem. Soc.* 111, 5852 (1989).
4. I. M. Tidswell, T. A. Rabedeau, P. S. Pershan, and S. D. Kosowsky, *J. Chem. Phys.* 95, 2854 (1991).
5. R. Banga, J. Yarwood, and A. M. Morgan, *Langmuir* 11, 4393 (1995).
6. A. Barrat, P. Silberzan, L. Bourdieu and D. Chatenay, *Europhysics Letters* 20, 633 (1992).
7. T. Nakagawa, K. Ogawa, and T. Kurumizawa, *Langmuir* 10, 525 (1994).
8. A. N. Parikh, B. Liedberg, S. V. Atre, M. Ho, and D. L. Allara, *J. Phys. Chem.* 99, 9996 (1995).
9. S. R. Cohen, R. Naaman, and J. Sagiv, *J. Phys. Chem.* 90, 3054 (1986).
10. D. K. Schwartz, S. Steinberg, J. Israelachvili, and J. A. N. Zasadzinski, *Phys. Rev. Lett.* 69, 3354 (1992).
11. K. Bierbaum, M. Grunze, A. A. Baski, L. F. Chi, W. Schrepp, and H. Fuchs, *Langmuir* 11, 2143 (1995).
12. Y. I. Rabinovich and R.-H. Yoon, *Langmuir* 10, 1903 (1994).
13. R. Banga, J. Yarwood, A. M. Morgan, B. Evans, and J. Kells, *Thin Solid Films* 284-285, 261 (1996).
14. D. L. Allara, A. N. Parikh, and E. Judge, *J. Chem. Phys.* 100, 1761 (1994).
15. D. W. Britt and V. Hlady, *J. Coll. Inter. Sci.* 178, 775 (1996).
16. D. L. Angst and G. W. Simmons, *Langmuir* 7, 2236 (1991).
17. D. H. Flinn, D. A. Guzonas, and R.-H. Yoon, *Colloids Surf. A* 87, 163 (1994).
18. T. Vallant, J. Kattner, B. H., U. Mayer, and H. Hoffmann, *Langmuir* 15, 5339 (1999).

19. R. Resch, M. Grasserbauer, G. Friedbacher, T. Vallant, H. Brunner, U. Mayer, and H. Hoffmann, *Applied Surface Science* 140, 168 (1999).
20. J. T. Woodward and D. K. Schwartz, *J. Am. Chem. Soc.* 118, 7861 (1996).
21. J. T. Woodward, A. Ulman, and D. K. Schwartz, *Langmuir* 12, 3626 (1996).
22. I. Doudevski, W. A. Hayes, and D. K. Schwartz, *Physical Review Letters* 81, 4927 (1998).
23. J. G. Amar and F. Family, *Physical Review Letters* 74, 2066 (1995).
24. I. Doudevski and D. K. Schwartz, *Physical Review B* 60, 14 (1999).
25. J. Als-Nielsen, D. Jacquemain, K. Kjaer, F. Leveiller, M. Lahav, and L. Leiserowitz, *Physics Reports* 246, 251 (1994).
26. Z. Nagy, H. You, and R. M. Yonco, *Rev. Sci. Instrum.* 65, 2199 (1994).
27. A.G. Richter, M.K. Durbin, C.J. Yu and P. Dutta, *Langmuir* 14, 5980 (1998)
28. A .G. Richter, C.J. Yu, A. Datta, J. Kmetko and P. Dutta, *Phys. Rev. E* 61, 607 (2000)
29. R. Banga, J. Yarwood, and A. M. Morgan, *Langmuir* 11, 618 (1995).
30. D. A. Styrkas, j. L. Keddie, J. R. Lu, and T. J. Su, *Journal of Applied Physics* 85, 868 (1999).
31. S. R. Wasserman, Y.-T. Tao, and G. M. Whitesides, *Langmuir* 5, 1074 (1989).
32. J. D. Le Grange, J. L. Markham, and C. R. Kurkjian, *Langmuir* 9, 1749 (1993).
33. J. B. Brzoska, N. Shahidzadeh, and F. Rondelez, *Nature* 360, 719 (1992).
34. P. Silberzan, L. Léger, D. Ausserré, and J. J. Benattar, *Langmuir* 7, 1647 (1991).
35. T. Vallant, H. Brunner, U. Mayer, H. Hoffmann, T. Leitner, R. Resch, and G. Friedbacher, *Journal of Physical Chemistry B* 102, 7190 (1998).
36. C. P. Tripp and M. L. Hair, *Langmuir* 8, 1120 (1992).
37. A. Eberhardt, P. Fenter, and P. Eisenberger, *Surface Science* 397, L285 (1998).
38. C. Carraro, O. W. Yauw, M. M. Sung, and R. Maboudian, *Physical Chemistry B* 102, 4441 (1998).

39. A. N. Parikh, M. A. Schivley, E. Koo, K. Seshadri, D. Aurentz, K. Mueller, and D. L. Allara, *J. Am. Chem. Soc.* 119, 3135 (1997)
40. C. P. Tripp and M. L. Hair, *Langmuir* 11, 1215 (1995).
41. D. L. Allara, A. N. Parikh, and F. Rondelez, *Langmuir* 11, 2357 (1995).

**Table I.** The time-offset Langmuir fit parameters (from ref. 28)

<b>Sample</b>	<b>Concentration</b> <b>(mM)</b>	<b><math>t_0</math></b> <b>(Hours)</b>	<b><math>\tau</math></b> <b>(Hours)</b>
S1	0.0025	$2.02 \pm 0.15$	$6.35 \pm 0.22$
S2	0.0025	$1.31 \pm 0.13$	$2.70 \pm 0.18$
S3	0.0025	0	$2.23 \pm 0.13$
S4	0.025	0	$1.19 \pm 0.03$
S9	0.15	0	$0.54 \pm 0.08$
S5	0.25	0	$1.40 \pm 0.16$

## FIGURE CAPTIONS

**Figure 1.** Simulated *in situ* reflectivity curves for a film with different solvents on top: heptane, toluene, and carbon tetrachloride. Note the absence of sharp features for toluene. Carbon tetrachloride would be a good choice of solvent because there is a large density contrast with an organic film; except that because it has a higher density, it will scatter more x-rays, increasing the background.

**Figure 2.** A schematic diagram of the *in situ* cell. The innermost piece is a Teflon slab with a cavity cut into it to hold the substrate and about 6 ml of solution. This is sandwiched between two beryllium plates that are nearly transparent to x-rays. This assembly is further sandwiched between two stainless steel pieces that provide structural support. The steel pieces have windows cut into them to pass the x-rays. The substrate surface is aligned with the lower edge of the windows.

**Figure 3.** An in-plane OTS monolayer diffraction peak, obtained under helium. The solid line is a Lorentzian fit.

**Figure 4.** LEFT: All the *in situ* reflectivity curves we obtained for samples S2, S3 and S5, deposited from various solution concentrations as marked. RIGHT: Coverage vs. time for the same samples; the solid lines are fits to the time-offset Langmuir model (parameters as marked).

**Figure 5.** The re-immersion experiment. Sample S7 was examined *in situ*, then removed from solution, rinsed, and scanned under helium. Finally, it was put back under clean heptane and scanned again. Sample S8 was in solution for the same amount of time as S7 and was not previously exposed to x-rays. S8 was scanned under clean heptane. The top graph is the reflectivities; the bottom is the electron density profiles. [From Ref. 28]

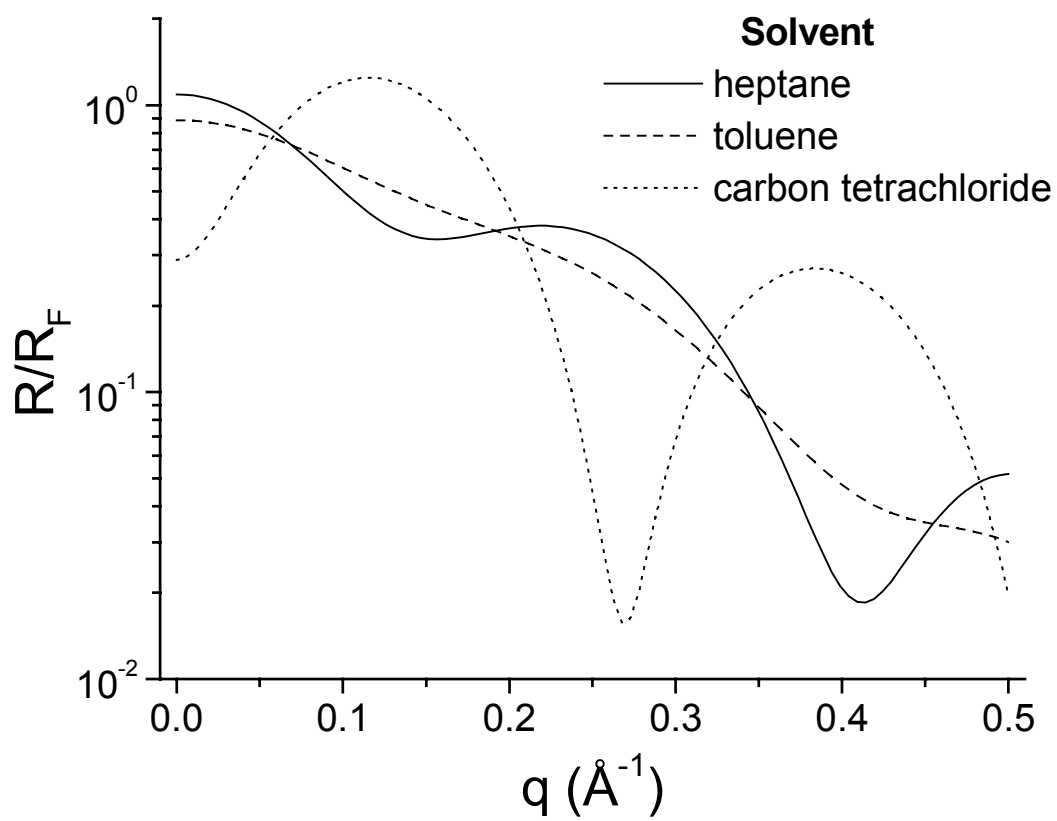


Fig. 1, Richter et al.

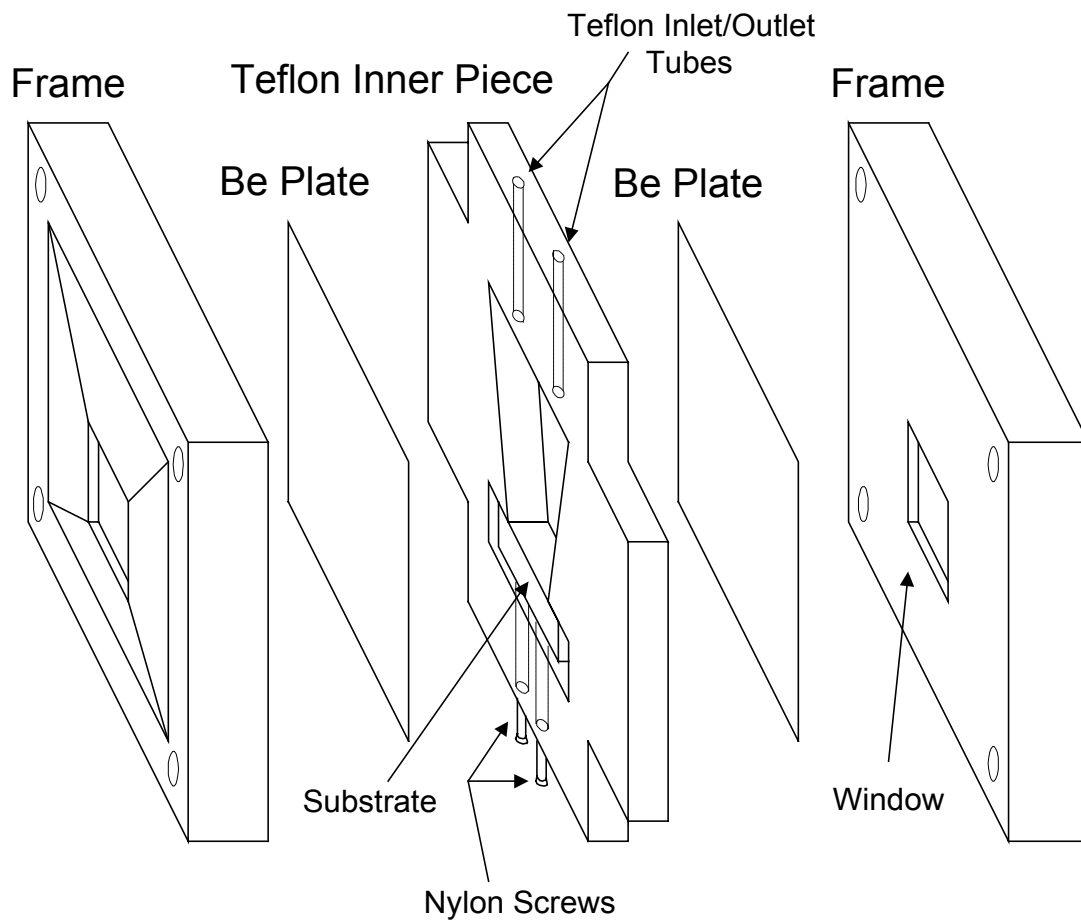


Fig. 2, Richter et al

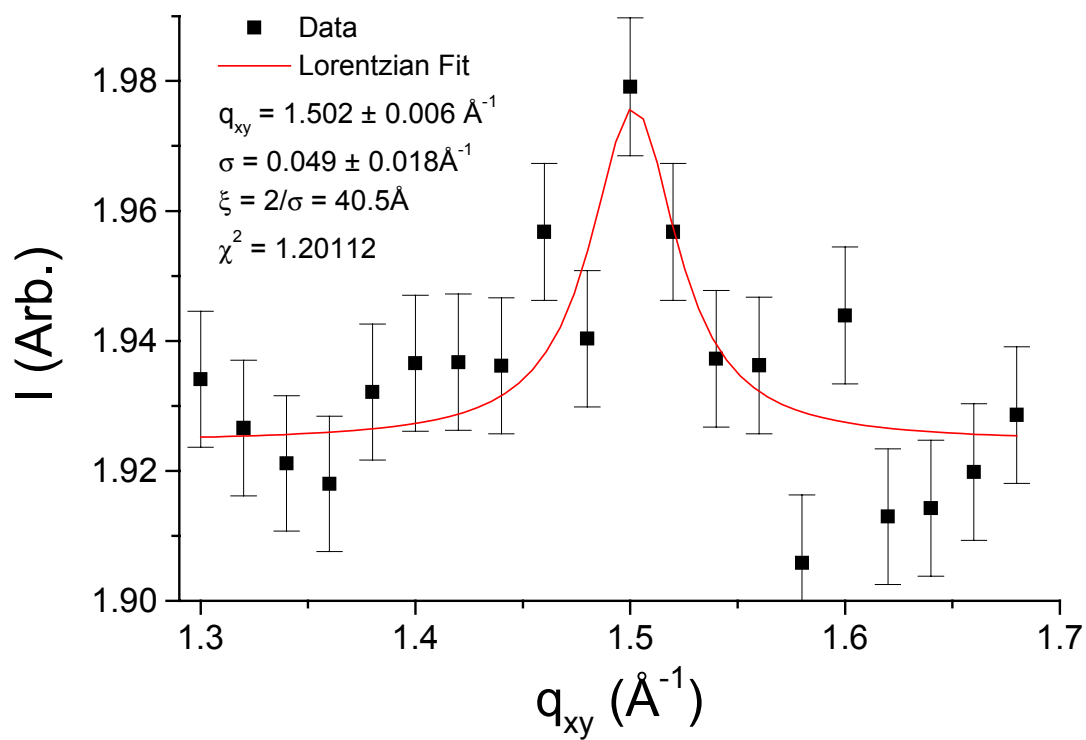


Fig. 3, Richter et al.

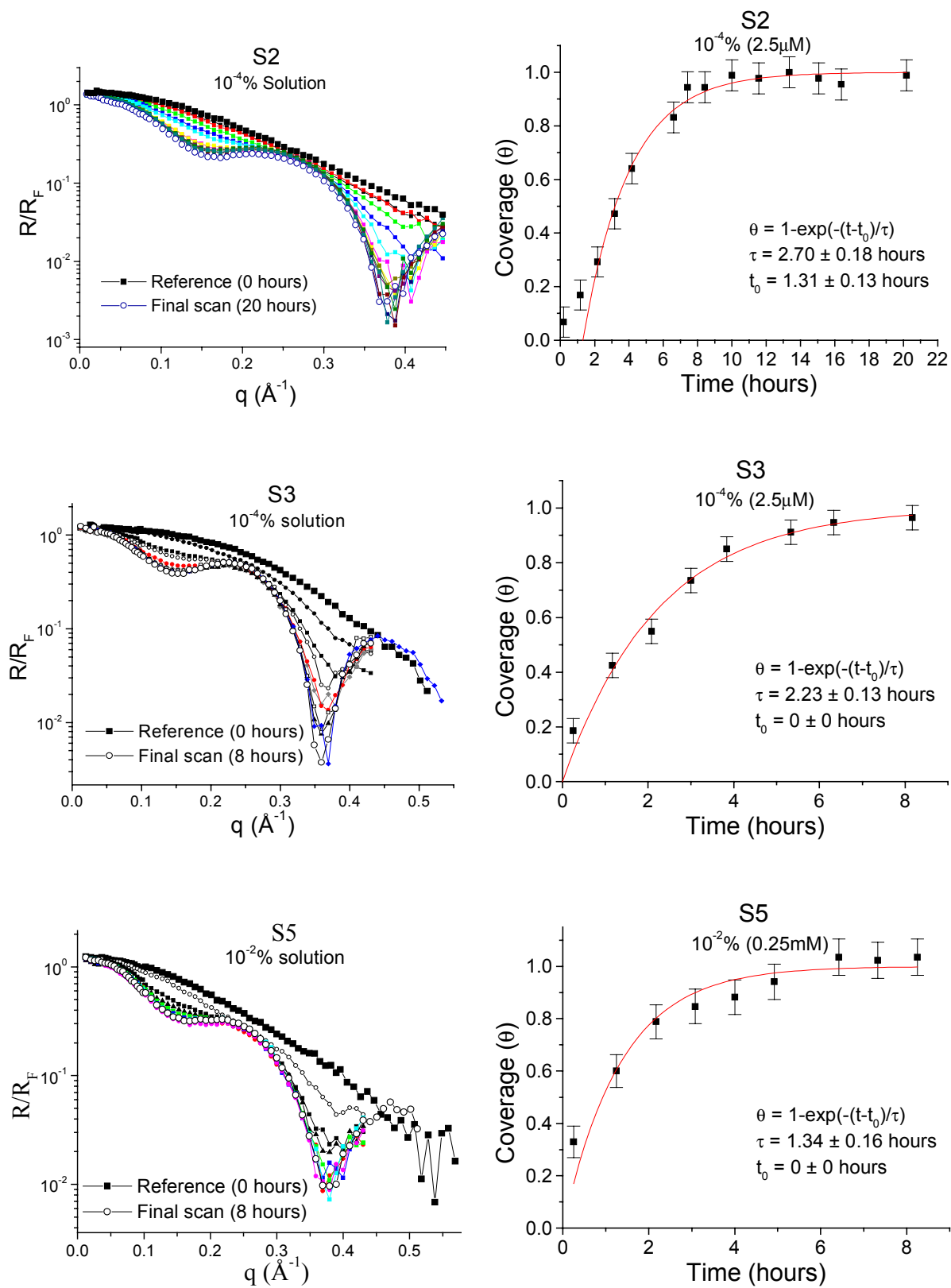


Fig. 4, Richter et al.

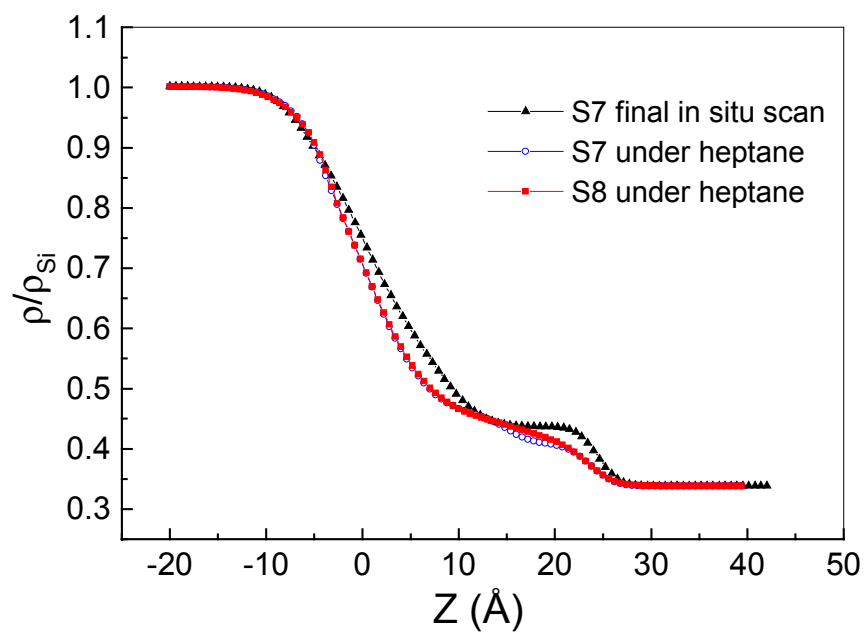
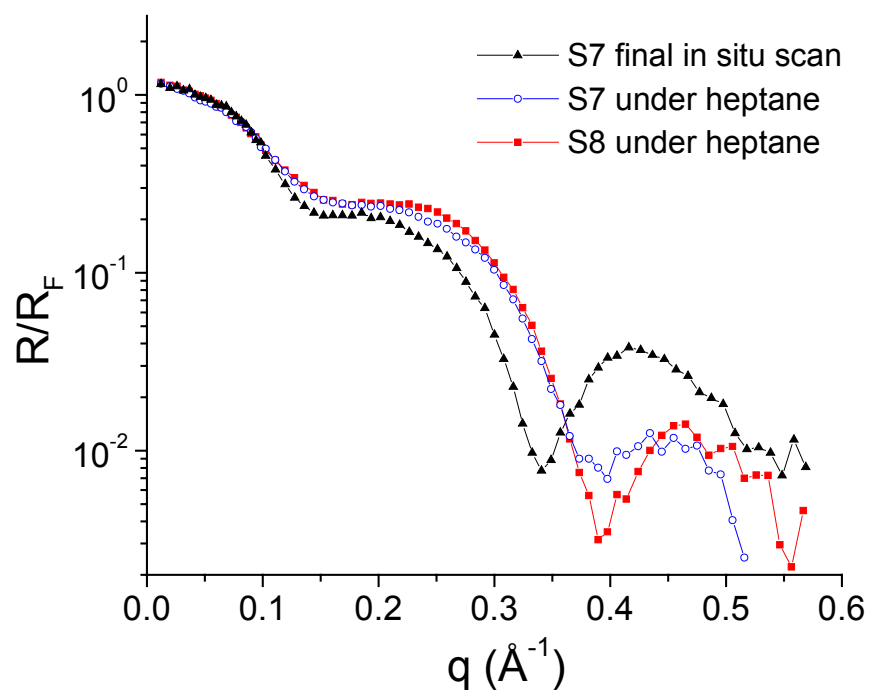


Fig. 5, Richter et al.